Estimation of Electronic Coupling for Intermolecular Electron Transfer from Cross-Reaction Data

Stephen F. Nelsen,* Michael N. Weaver, and Yun Luo

Department of Chemistry, University of Wisconsin, Madison, Wisconsin 53706-1396

Jack R. Pladziewicz,* Logan K. Ausman, Teresa L. Jentzsch, and Jessica J. O'Konek

Department of Chemistry, University of Wisconsin, Eau Claire, Wisconsin 54702-4004

Received: July 12, 2006

Sixty-five electron-transfer reactions including 27 new 0, +1 couples have been added to our data set of cross-reactions between 0 and +1 couples, bringing it to 206 reactions involving 72 couples that have been studied by stopped-flow kinetics in acetonitrile containing supporting electrolyte at 25 °C, formal potentials determined by cyclic voltammetry, and analyzed using Marcus cross-rate theory. Perhaps surprisingly, a least-squares analysis demonstrates that intrinsic rate constants exist that predict the cross-rate constants to within a factor of 2 of the observed ones for 93% of the reactions studied, and only three of the reactions have a cross-rate constant that lies outside of the factor of 3, that corresponds to a factor of 10 uncertainty in the rate constant for an unknown couple. Many triarylamines, which have very high intrinsic reactivity, are included among the newly studied couples. The enthalpy contribution to the Marcus reorganization energy, λ'_v, has been calculated for 46 of the couples studied, at the (U)B3LYP/6-31+G* (or for the larger and lower barrier compounds, at the less time-consuming (U)B3LYP/6-31G*) level. In combination with a modified Levich and Dogodnadze treatment that assumes that the rate constant is proportional to $(K_e H_{ab}^2/\lambda^{1/2}) \exp[-\Delta G^*/RT]$, this allows estimation of the electronic coupling (H_{ab}) at the transition state for intermolecular electron transfer, (more properly H'_{ab}, the product of the square root of the encounter complex formation constant times H_{ab}) for these couples. Although the principal factor affecting intermolecular electron-transfer rate constants is clearly λ, H'_{ab} effects are easily detectable, and the dynamic range in our estimates of them is over a factor of 600.

Introduction

The principal result of classical Marcus cross-reaction theory[1] is that the only factors that affect intermolecular electron transfer (ET) reactivity are the intrinsic "self-reaction" rate constants for the couples, k_{ii} and k_{jj}, and the equilibrium constant for the reaction, K_{ij}. For ET between the 0, +1 couples that we consider here, where there are no "work terms", the result is the exceptionally simple eq 1. If eq 1 is useful, only knowing k_{ii}

$$k_{ij}(\text{calcd}) = (k_{ii}k_{jj}K_{ij}f_{ij})^{1/2} \tag{1}$$

$$\ln(f_{ij}) = [\ln(K_{ij})]^2/[4\ln(k_{ii}k_{jj}/Z^2)] \tag{1a}$$

and the related $E^{\circ\prime}$ value will produce the reaction rate constant k_{ij} with all other couples for which k_{ii} and $E^{\circ\prime}$ are also known. Equation 1 seems to be little more than writing down "How simple could it be?", and it apparently should not work in the light of modern theory. Marcus had assumed that intermolecular ET reactions were adiabatic in deriving eq 1, and it is now generally accepted that they are nonadiabatic.[2] Adiabatic reactions in principle have only slightly different pre-exponential factors, and the basis of cross-rate theory was that one only needed to consider the effect of the exponential term containing ΔG^* and that averaging the barriers would be sufficient to accurately predict the cross-reaction rate constant. Nonadiabatic reactions ought to have pre-exponential factors that vary widely with structure, which would make eq 1 fail.

One of the most puzzling aspects of intermolecular electron transfer has always been how to estimate what the electronic coupling, the H_{ab} of Marcus theory, is. Nonadiabatic reactions have $(H_{ab})^2$ in their pre-exponential term as well as affecting the exponential term of the rate constant.[1,2] Although a basic assumption of the two-state model is that H_{ab} is a single constant, it obviously changes with distance and relative orientation of the reactants for an intermolecular electron transfer. Two molecules can approach each other in a plethora of ways, and the electronic coupling at the transition state is going to be sensitive to how effective the contact is between the molecules. One might therefore suppose that H_{ab} for a cross-reaction between two different ET partners would be very sensitive to the reaction partner and significantly different from that of the related self-exchange reactions. The problem with expecting a classical theory to work is especially brought out using Jortner's popular kinetic treatment of ET reactions,[2] often called the Golden Rule equation.[3,4] It replaces Marcus's exponential term $e^{(-\Delta G^*/RT)}$ with Franck−Condon tunneling factors. Then, the ratio of the "averaged barrier crossing frequency", which we will call $h\nu_v$, to the internal vibrational part of the reorganization energy, λ_v, usually called S, is a fundamentally important parameter. Because e^{-S} (as well as $(H_{ab})^2$) then appears in the pre-exponential factor, and S varies by an order of magnitude between high λ_v compounds, such as hydrazines, and low λ_v ones, such as aromatics, it is even clearer that Marcus cross-rate theory using a constant pre-exponential factor should not work.

10.1021/jp064406v CCC: $33.50
Published on Web 09/26/2006

The hypothesis of eq 1 that only the difference in oxidation potential and a single intrinsic rate constant for each couple will predict the rate constants of cross-reactions is testable, and we have carried out extensive studies for mostly organic couples.[5−11] We were surprised to discover that using eq 1 to analyze observed rate constants works quite quantitatively for essentially all of the reactions that we have studied. The same k_{ii}(fit) values allow calculation of cross-rate constants k_{ij} to comparable accuracy regardless of the S values of the couples involved, so the expected effect of the e^{-S} term is not observed experimentally. That is, a single, consistent k_{ii}(fit) value is obtained for a particular couple that allows accurate estimation of cross-reaction rate constants for reactions with both very low and very high barrier compounds. The k_{ii}(fit) values obtained vary over a range of 10^{14}, so intrinsic ET reactivity is exceptionally sensitive to structure. The principal factor controlling k_{ii}(fit) is clearly the internal reorganization energy, Marcus's λ_v. We calculate the enthalpy contribution to λ_v (which we call λ'_v) using the simple method that we introduced.[12] If E is the enthalpy calculated for an oxidation level of a couple, **n** and **c** correspond to the optimized geometry of the neutral and cation oxidation levels of the couple, respectively, and the charge present for the calculation is shown as a superscript (0 for neutral, + for radical cation), λ'_v may be calculated by eq 2

$$\lambda'_v = [E(\mathbf{c}^0) - E(\mathbf{n}^0)] + [E(\mathbf{n}^+) - E(\mathbf{c}^+)] \qquad (2)$$

However, as we have just argued, people no longer expect the pre-exponential terms for electron-transfer reactions to be constant, as Marcus had assumed in deriving cross-rate theory. For eq 1 to work as well as it does, averaging the pre-exponential terms for cross-reactions is apparently as good an assumption as averaging the barriers, although we have seen no one predict that this would be the case. We suggested earlier that a plausible interpretation of the observed k_{ii}(fit) values is that the pre-exponential factor indeed contains $(H_{ab})^2$.[10] In this work, we report an additional 65 reactions and 27 new couples, studied under the same conditions as the previous reactions. Many of these are for very low barrier compounds, such as triarylamines. The more reliable λ'_v values calculated here are used to discuss intrinsic H_{ab} values from our experimental data for cases that are conformationally simpler.

Results

We have previously described our methodology, which involves measuring cross-reaction rate constants (k_{ij}) under pseudo-first-order conditions in acetonitrile containing 0.1 M tetrabutylammonium perchlorate at 25 °C using stopped-flow spectrophotometry for as many cross-reactions as practical for each compound in the set. K_{ij} is obtained by combining the relevant $E^{\circ\prime}$ values, obtained with the same solvent, ionic composition, and temperature, using cyclic voltammetry. The entire set of experimental k_{ij} values is simultaneously fit to eq 1 using the experimental K_{ij} values and Z fixed at 1×10^{11} M^{-1} s^{-1} employing a least-squares routine.[8] Marcus's original value of $Z = 10^{11}$ has been retained, because it makes little difference within a couple of orders of magnitude what value is used to analyze our data set.[6] The most recent data set we published included 141 reactions involving 45 couples.[10] We have now enlarged our data set to 206 reactions involving 72 couples and have especially emphasized obtaining more data relating to faster ET couples. The structures of the 27 previously unstudied couples, with acronyms and numbers that correspond to the compound numbers in the table of reactions studied (see Experimental Section) appear in Chart 1, and those of the 16 previously studied couples that were crossed with them to obtain the cross-rate data are shown in Chart 2. Chart 3 contains the structures of 19 additional couples for which λ'_v calculations have been carried out in this work. The summary of k_{ii}(fit) and $\Delta G^{\ddagger}_{ii}$(fit) values for the 62 couples considered here appears as Table 1. Fewer cross-reactions for each new couple have been run to establish $\Delta G^{\ddagger}_{ii}$ for many of the newer compounds added to the data set because we have established[5−10] that stable values are obtained from measuring 3−4 cross-reaction rate constants for a particular couple. This has allowed us to focus our efforts on examining a wider range of couples.

We have also carried out hybrid Hartree−Fock, density functional theory calculations, (U)B3LYP of the internal vibrational reorganization energy, λ'_v, for many of the couples studied; see eq 2 above. For convenience, we will refer to these as DFT calculations. Table 2 repeats the intrinsic Eyring barriers, $\Delta G^{\ddagger}_{ii}$(fit), and summarizes the λ'_v(DFT) values that we have calculated, as well as the electronic coupling derived from it. The couples in Table 2 are arranged in a very different order from that of Table 1, that of increasing intrinsic H'_{ab} value (see discussion).

Discussion

1. k_{ii}(fit) Values. The k_{ii}(fit) values of Table 1 unquestionably have experimental significance. They let one calculate k_{ij} rather accurately, in the overwhelming majority of cases to within a factor of 2 of the observed value. 92% of the 206 reactions studied have k_{ij}(calcd) values that lie within a factor of 2 of k_{ij}(obsd); that is, they have k_{ij}(obsd)/k_{ij}(calcd) ratios that lie in the range 0.5−2.0. Only three of the reactions studied have k_{ij}(calcd) using the k_{ii}(fit) values of Table 1 that deviate more than a factor of 3 from k_{ij}(obsd) and thus lie outside the $10^{-1/2}$ to $10^{1/2}$ (0.32 to 3.16) range that represents a factor of 10 in k_{ii}(fit) for an unknown couple. Nine of the couples discussed here have only had one reaction studied (see the last two columns of Table 1). For the others, the root-mean-square deviation of $\Delta G^{\ddagger}$ for each reaction from $\Delta G^{\ddagger}_{ii}$(fit) is listed in the last column. Their average is 0.22 kcal/mol, and only four couples (**nPr$_4$N$_4^{0/+}$**(58/1) at 0.72 kcal/mol, **An$_3$N$^{0/+}$**(56/1) at 0.61, **Xy$_2$pBrN$^{0/+}$**(63/1) at 0.49, and **33)$_2$N$_4^{0/+}$**(35/2) at 0.42) have root-mean-square deviations larger than twice this value. We cannot suggest why these couples behave less well than the others; well-behaved couples that have only small structural differences are also present in the data set. It seems likely that mistakes would creep into a large data set, but we have been unable to determine that anything is "wrong" experimentally with the deviant reactions. It appears from these comparisons that $\Delta G^{\ddagger}_{ii}$(fit) is determined to approximately 0.3 kcal/mol for most reactions by these experiments. We have previously discussed the relationship of k_{ii}(fit) values to known self-exchange rate constants[6,11] and will not repeat the discussion here. The majority of the couples cannot be studied under self-exchange reaction conditions, because they are too slow (NMR line broadening becomes too small to give accurate results for $k_{ex} < \sim 700$ M^{-1} s^{-1}, and diffusion limits accuracy when k_{ex} is above about 10^9 M^{-1} s^{-1}).

2. λ'_v Calculations. In previous papers, we used semiempirical AM1 calculations to correlate our data. When only small structural changes are involved in a series of couples to be compared, AM1 calculations predict reactivity changes in this series rather well, but they do not allow comparison of compounds of different sorts quantitatively. In this work, we shall assume that DFT calculations produce usefully accurate

CHART 1: Structures of the 27 Previously Unstudied Couples

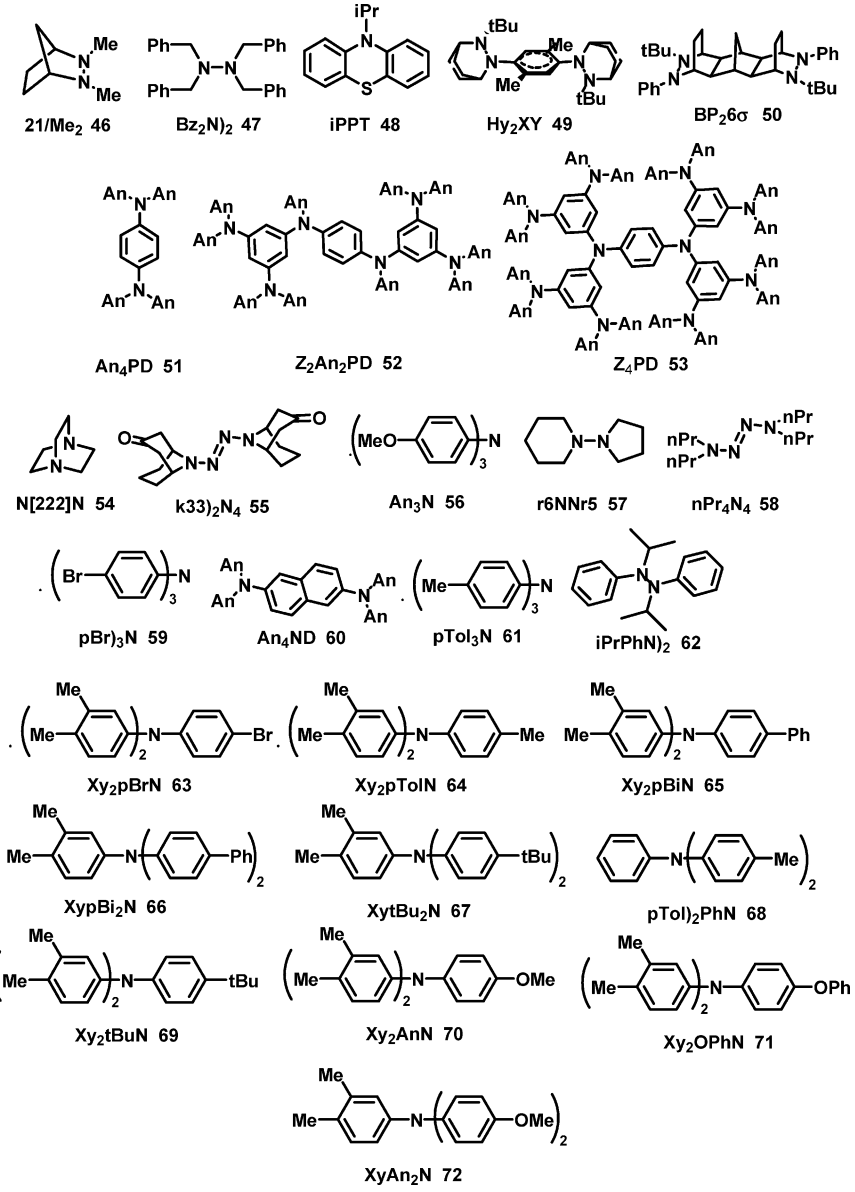

CHART 2: Structures of 16 Previously Studied Couples Used to Obtain the Cross-Rate Data for the Couples of Chart 1

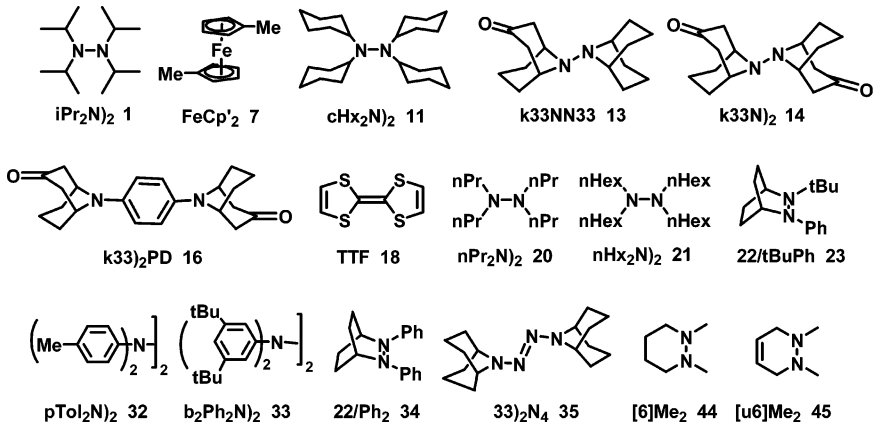

λ'_v values for the compounds studied and not consider AM1 calculations further.

The very high $\Delta G^{\ddagger}_{ii}$(fit) values observed for tetra-*n*-alkyl hydrazines make it quite clear that only energy-minimum conformations need to be considered in estimating λ'_v. If non-minimum-energy conformations had been available for electron-transfer reactions, the far smaller λ'_v values for conformations with the lone pair, lone pair twist angle θ larger than the minimum-energy value that is near 90° would have resulted in far faster electron-transfer reactions than observed. The difficulty in calculating λ'_v for a couple depends greatly upon its structure. When energy minima for many different conformations are

CHART 3: Structures of 19 Additional Couples for Which λ'_v and H'_{ab} Calculations Are Reported

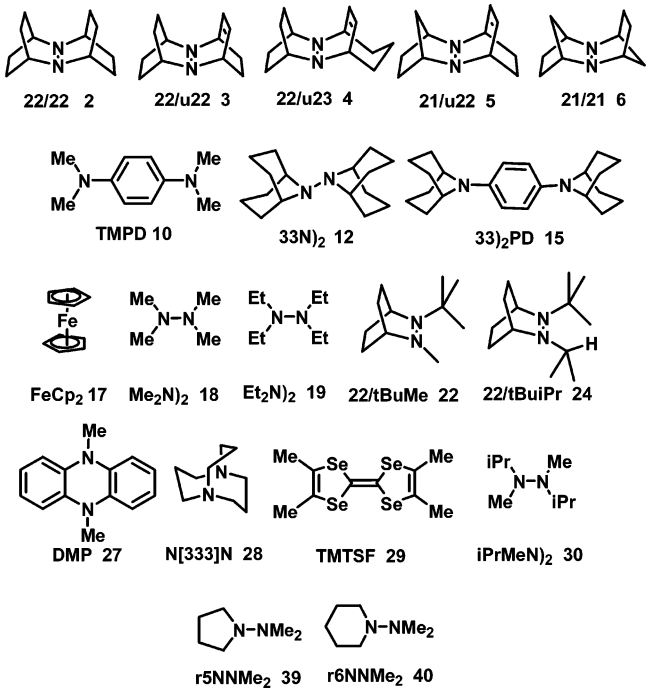

present for both the neutral form and the radical cation of a couple, each pair of minima in principle produces a different λ'_v value.

Hydrazines with alkyl groups that can undergo internal rotations have many minima on their energy surfaces. For considering how this complexity should affect their kinetics for self-ET, we will consider **iPr$_2$N)$_2^{0/+}$** and **Et$_2$N)$_2^{0/+}$** in some detail. Both the neutral form and radical cation conformations affect λ'_v, but here we just consider the energy surface for the neutral forms, which we believe are the most important because of the lower barrier to changing the NN twist angle θ, which we expect to allow more minima, and because the cation relaxation energy and hence λ'_v is quite sensitive to changes in θ. Molecular mechanics searches using *Spartan '02* gave 19 and 39 energy minima, respectively, that lie within 10 kcal/mol of the global minimum for **iPr$_2$N)$_2^0$** and **Et$_2$N)$_2^0$**. Each of these structures was geometry-optimized at B3LYP/6-31G*, producing a series of $\mathbf{n}^0$ structures and energies, and after CNG calculations on each, a series of $\mathbf{n}^+$ energies; see Table 3. These were combined with the $\mathbf{c}^+$ and $\mathbf{c}^0$ values for the lowest-energy $\mathbf{c}^+$ structure[13] to produce $\lambda'_v(i)$ values corresponding to each neutral structure. Rate constants at 298 K relative to those for the most stable neutral conformation (labeled $i = 1$), assuming that λ'_v change is the only factor affecting the rate constant, were calculated, using $k_{rel} = \exp(-[\lambda'_v(i) - \lambda'_v(1)]/4RT)$. Because conformational interconversions are limited by alkyl group rotations, they ought to be fast compared to the intermolecular electron-transfer rate, so the contribution of each conformer to the observed rate should be given by the Boltzmann factor that weights the amounts of these conformations at equilibrium, $\exp(-[E(\mathbf{n}^0_i) - E(\mathbf{n}^0_1)]/RT)$, shown in the second to the last column as $e^{-\Delta E(i)/RT}$. The last column shows the fraction of material calculated to proceed through each neutral conformation, $f(i) = k_{rel}(i)\, e^{-\Delta E(i)/RT}/\sum_i[k_{rel}(i)\, e^{-\Delta E(i)/RT}]$. The pattern of contributing neutral conformations obtained is very different for these two couples; see Figure 1. **iPr$_2$N)$_2^{0/+}$**

TABLE 1: Results of the 206 Reaction Data Set Analysis for the 62 Couples Considered in This Paper, Arranged in Decreasing Order of $\Delta G^{\ddagger}_{ii}$(fit) (increasing ET Reactivity)

structure/ chart	couple	$E^{\circ\prime}$/ V	k_{ii}(fit)/ $M^{-1}s^{-1}$	$\Delta G^{\ddagger}_{ii}$ (fit)	reactions studied	rms devn[a]	structure/ chart	couple	$E^{\circ\prime}$/ V	k_{ii}(fit)/ $M^{-1}s^{-1}$	$\Delta G^{\ddagger}_{ii}$ (fit)	reactions studied	rms devn[a]
20/2	**nPr$_2$N)$_2^{0/+}$**	0.29	4.5×10^{-4}	22.0	10	0.12	55/1	**k33)$_2$N$_4^{0/+}$**	0.75	7.2×10^{4}	10.8	4	0.14
19/3	**Et$_2$N)$_2^{0/+}$**	0.29	5.3×10^{-4}	21.9	3	0.16	35/2	**33)$_2$N$_4^{0/+}$**	0.40	8.0×10^{5}	9.4	10	0.48
21/2	**nHx$_2$N)$_2^{0/+}$**	0.29	1.3×10^{-3}	21.4	5	0.19	58/1	**nPr$_4$N$_4^{0/+}$**	0.35	1.9×10^{6}	8.9	3	0.72
30/3	**iPrMeN)$_2^{0/+}$**	0.24	1.4×10^{-3}	21.4	3	0.28	7/2	**FeCp'$_2^{0/+}$**	0.281	5.1×10^{6}	8.3	4	0.16
1/2	**iPr$_2$N)$_2^{0/+}$**	0.26	2.7×10^{-3}	21.0	29	0.23	33/2	**b$_2$Ph$_2$N)$_2^{0/+}$**	0.61	8.0×10^{6}	8.0	7	0.42
47/1	**Bz$_2$N)$_2^{0/+}$**	0.60	3.6×10^{-3}	20.8	15	0.18	17/3	**FeCp$_2^{0/+}$**	0.395	1.3×10^{7}	7.7	4	0.13
11/2	**cHx$_2$N)$_2^{0/+}$**	0.26	2.5×10^{-2}	19.6	27	0.29	16/2	**k33)$_2$PD$^{0/+}$**	0.29	4.0×10^{7}	7.1	21	0.24
45/2	**[u6]Me$_2^{0/+}$**	0.28	8.0×10^{-2}	19.0	7	0.40	68/1	**pTol)$_2$PhN$^{0/+}$**	~.812	1.0×10^{8}	~6.5	1	
18/3	**Me$_2$N)$_2^{0/+}$**	0.28	1.7×10^{-1}	18.5	3	0.29	10/3	**TMPD$^{0/+}$**	0.12	1.1×10^{8}	6.5	8	0.15
40/3	**r6NNMe$_2^{0/+}$**	0.31	4.0×10^{-1}	18.0	2	0.23	63/1	**Xy$_2$pBrN$^{0/+}$**	0.85	1.0×10^{8}	6.5	3	0.49
39/3	**r5NNMe$_2^{0/+}$**	0.12	5.8×10^{-1}	17.8	3	0.44	53/1	**Z$_4$PD$^{0/+}$**	0.51	1.2×10^{8}	6.4	3	0.08
57/1	**r6NNr5$^{0/+}$**	0.15	9.3×10^{-1}	17.5	2	0.33	15/3	**33)$_2$PD$^{0/+}$**	0.02	1.6×10^{8}	6.3	3	0.33
46/1	**21/Me$_2^{0/+}$**	0.15	1.4×10^{0}	17.3	5	0.23	59/1	**pBr)$_3$N$^{0/+}$**	1.10	2.7×10^{8}	5.9	1	
44/2	**[6]Me$_2^{0/+}$**	0.18	4.9×10^{0}	16.5	4	0.24	32/2	**pTol$_2$N)$_2^{0/+}$**	0.65	6.4×10^{8}	5.4	4	0.20
24/3	**22/tBuiPr$^{0/+}$**	0.10	1.5×10^{1}	15.8	3	0.22	27/3	**DMP$^{0/+}$**	0.138	8.2×10^{8}	5.3	7	0.17
14/2	**k33N)$_2^{0/+}$**	0.45	2.6×10^{1}	15.5	20	0.22	71/1	**Xy$_2$OPhN$^{0/+}$**	0.723	8.3×10^{8}	5.3	2	0.00
22/3	**22/tBuMe$^{0/+}$**	0.11	4.6×10^{1}	15.2	3	0.10	61/1	**pTol$_3$N$^{0/+}$**	0.775	1.1×10^{9}	5.1	6	0.12
28/3	**N[333]N$^{0/+}$**	0.165	4.9×10^{1}	15.2	3	0.24	72/1	**XyAn$_2$N$^{0/+}$**	0.602	1.2×10^{9}	5.1	1	
2/3	**22/22$^{0/+}$**	−0.53	9.6×10^{1}	14.7	2	0.15	69/1	**Xy$_2$tBuN$^{0/+}$**	0.739	1.2×10^{9}	5.1	2	0.07
13/2	**k33NN33$^{0/+}$**	0.22	2.2×10^{2}	14.3	13	0.15	51/1	**An$_4$PD$^{0/+}$**	0.35	1.2×10^{9}	5.1	6	0.26
12/3	**33N)$_2^{0/+}$**	−0.01	7.1×10^{2}	13.6	11	0.20	52/1	**Z$_2$An$_2$PD$^{0/+}$**	0.49	1.3×10^{9}	5.0	4	0.24
5/3	**21/u22$^{0/+}$**	0.058	1.0×10^{3}	13.3	9	0.18	67/1	**XytBu$_2$N$^{0/+}$**	0.766	1.3×10^{9}	5.0	2	0.00
23/2	**22/tBuPh$^{0/+}$**	0.26	1.1×10^{3}	13.3	6	0.06	64/1	**Xy$_2$pTolN$^{0/+}$**	0.73	1.4×10^{9}	5.0	1	
3/3	**22/u22$^{0/+}$**	−0.241	1.2×10^{3}	13.2	5	0.21	48/1	**iPPT$^{0/+}$**	0.737	1.3×10^{9}	5.0	1	
4/3	**22/u23$^{0/+}$**	−0.298	2.4×10^{3}	12.8	3	0.11	70/1	**Xy$_2$AnN$^{0/+}$**	0.653	1.7×10^{9}	4.9	3	0.07
6/3	**21/21$^{0/+}$**	0.01	3.2×10^{3}	12.7	4	0.12	65/1	**Xy$_2$pBiN$^{0/+}$**	0.77	3.3×10^{9}	4.4	3	0.12
49/1	**Hy$_2$XY$^{0/+}$**	0.03	5.3×10^{3}	12.4	2	0.08	66/1	**XypBi$_2$N$^{0/+}$**	0.823	4.0×10^{9}	4.3	1	
54/1	**N[222]N$^{0/+}$**	0.58	7.3×10^{3}	12.2	1		18/2	**TTF$^{0/+}$**	0.33	1.6×10^{10}	3.5	15	0.27
50/1	**BP$_2$6$\sigma^{0/+}$**	0.185	1.3×10^{4}	11.8	1		60/1	**An$_4$ND$^{0/+}$**	0.456	1.6×10^{10}	3.5	4	0.18
62/1	**iPrPhN)$_2^{0/+}$**	0.70	4.4×10^{4}	11.1	1		56/1	**An$_3$N$^{0/+}$**	0.56	2.3×10^{10}	3.3	2	0.61[b]
34/2	**22/Ph$_2^{0/+}$**	0.48	5.6×10^{4}	11.0	13	0.33	29/3	**TMTSF$^{0/+}$**	0.424	1.6×10^{11}	2.2	13	0.18

[a] rms devn = $[\sum(\text{devn})^2/n]^{1/2}$, with single reaction couples not included in n, where devn is the difference between $\Delta G^{\ddagger}$ calculated for each reaction of the couple and their average, $\Delta G^{\ddagger}_{ii}$(fit). [b] The two reactions studied give incompatible rate constants (see Discussion section).

TABLE 2: Observed $\Delta G^{\ddagger}_{ii}$(fit), (U)B3LYP λ'_v, and H'_{ab} Resulting from Using $\Delta G^{*}_s = 2$[a]

structure/ chart	couple	$\Delta G^{\ddagger}_{ii}$(fit)	λ'_v(DFT)[b]	H'_{ab} ($\Delta G^{*}_s = 2.0$)	structure/ chart	couple	$\Delta G^{\ddagger}_{ii}$(fit)	λ'_v(DFT)[b]	H'_{ab} ($\Delta G^{*}_s = 2.0$)
28/3	**N[333]N$^{0/+}$**	15.2	23.70	0.001	32/2	**pTol$_2$N)$_2^{0/+}$**	5.4	5.18	0.06
54/1	**N[222]N$^{0/+}$**	12.2	16.07	0.003	46/1	**21/Me$_2^{0/+}$**	17.3	50.94,51.97	0.07, 0.08
17/3	**FeCp$_2^{0/+}$**	7.7	4.51[c]	0.008[c]	4/3	**22/u23$^{0/+}$**	12.8	33.84,34.37	0.07, 0.08
33/2	**b$_2$Ph$_2$N)$_2^{0/+}$**	8.0	7.70	0.01	34/2	**22/Ph$_2^{0/+}$**	11.0	26.67,27.53	0.07, 0.08
47/1	**Bz$_2$N)$_2^{0/+}$**	20.8	57.83	0.02	12/3	**33N)$_2^{0/+}$**	13.6	37.58,38.15	0.08, 0.09
2/3	**22/22$^{0/+}$**	14.7	37.09	0.03	65/1	**Xy$_2$pBiN$^{0/+}$**	4.4	2.94	0.09
23/2	**22/tBuPh$^{0/+}$**	13.3	30.00, 31.19	0.02, 0.03	70/1	**Xy$_2$AnN$^{0/+}$**	4.9	4.63	0.09
62/1	**iPrPhN)$_2^{0/+}$**	11.1	20.79	0.02	51/1	**An$_4$PD$^{0/+}$**	5.1	5.66	0.10
63/1	**Xy$_2$pBrN$^{0/+}$**	6.5	3.21	0.02	6/3	**21/21$^{0/+}$**	12.7	36.49,37.54	0.14, 0.17
30/3	**iPrMeN)$_2^{0/+}$**	21.4	63.89,64.69	0.03, 0.04	10/3	**TMPD$^{0/+}$(syn)**	6.5	12.92, 12.50	0.15, 0.14
3/3	**22/u22$^{0/+}$**	13.2	32.10,32.88	0.03, 0.04	55/1	**k33)$_2$N$_4^{0/+}$**	10.8	30.93	0.20
44/2	**[6]Me$_2^{0/+}$(ee)**	16.5	43.88,46.91	0.03, 0.05	16/2	**k33)$_2$PD$^{0/+}$**	7.1	17.79	0.27
24/3	**22/tBuiPr$^{0/+}$**	15.9	42.01,42.34	0.03, 0.03	27/3	**DMP$^{0/+}$**	5.3	11.34, 8.91	0.29, 0.17
59/1	**pBr)$_3$N$^{0/+}$**	5.9	3.17	0.03	18/3	**Me$_2$N)$_2^{0/+}$**	18.5	62.55, 64.95	0.29, 0.48
14/2	**k33N)$_2^{0/+}$**	15.5	40.03,40.20	0.03, 0.03	40/3	**r6NNMe$_2^{0/+}$**	18.0	61.20, 62.85	0.32, 0.46
45/2	**[u6]Me$_2^{0/+}$(ae)**	19.0	55.01,58.08	0.04, 0.07	39/3	**r5NNMe$_2^{0/+}$**	17.8	63.67, 64.49	0.61, 0.78
5/3	**21/u22$^{0/+}$**	13.3	34.40,35.18	0.05, 0.06	48/1	**iPTT$^{0/+}$**	5.0	10.64	0.32
22/3	**22/tBuMe$^{0/+}$**	15.2	41.25,42.23	0.05, 0.06	60/1	**An$_4$ND$^{0/+}$**	3.5	5.45	0.34
19/3	**Et$_2$N)$_2^{0/+}$**	21.9	67.92,69.71	0.05, 0.07	15/3	**33)$_2$PD$^{0/+}$**	6.3	15.98	0.37
1/2	**iPr$_2$N)$_2^{0/+}$**	21.0	64.90,61.80	0.06,0.03	18/2	**TTF$^{0/+}$**	3.5	6.12, 7.58	0.41, 0.58
61/1	**pTol$_3$N$^{0/+}$**	5.1	2.92	0.05	35/2	**33)$_2$N$_4^{0/+}$**	9.4	28.72	0.42
64/1	**Xy$_2$pTolN$^{0/+}$**	5.0	2.98	0.05	56/1	**(An)$_3$N$^{0/+}$**	3.3[d]	6.28	0.50
69/1	**Xy$_2$tBuN$^{0/+}$**	5.1	2.99	0.05	29/3	**TMTSF$^{0/+}$**	2.2	3.40, [9.79][e]	0.68, [2.99][e]

[a] Energies are in kcal/mol. Couples are listed in order of increasing H'_{ab}. [b] From (U)B3LYP/6-31+G(d) calculations if not marked, and for cases marked (U)B3LYP/6-31G(d). [c] From (U)B3LYP/LACV3P** calculations using *Jaguar*. [d] The barrier is probably too low; the H'_{ab} it gives is anomalously high (see text). [e] See text for discussion of why the numbers in brackets are anomalous.

TABLE 3: Energies (kcal/mol) of iPr$_2$N)$_2^{0/+}$ and Et$_2$N)$_2^{0/+}$ Conformations Contributing to Self-ET

i	$E(\mathbf{n}^0_i) - E(\mathbf{n}^0_1)$	$E(\mathbf{n}^+_i) - E(\mathbf{n}^+_1)$	$\Delta H_r(i)$ (cat)	$\Delta H_r(i)$ (neu)	$\lambda'_v(i)$	$k_{rel}(i)$	$e^{-\Delta E(i)/RT}$	$f(i)$
			iPr$_2$N)$_2^{0/+}$					
			λ'_v(eff) = 61.1					
1	≡0	≡0	23.34	38.22	61.56	1	1	0.810
2	1.69	−0.37	22.97	36.53	59.50	2.4	0.058	0.111
3	2.20	−0.74	22.60	36.02	58.62	3.5	0.024	0.068
			Et$_2$N)$_2^{0/+}$					
			λ'_v(eff) = 67.7					
1	≡0	≡0	32.49	37.56	70.05	≡1	≡1	0.591
2	2.71	−2.84	29.64	34.85	64.49	10.4	0.010	0.063
3	2.27	−1.43	31.05	35.29	66.34	4.78	0.021	0.061
4	2.27	−1.07	31.41	35.29	66.70	4.10	0.022	0.053
5	3.70	−3.89	28.60	33.86	62.46	24.6	0.002	0.028
6	2.32	0.32	32.80	35.24	68.05	2.32	0.020	0.027
7	4.61	−6.24	26.25	32.95	59.20	97.4	4×10^{-4}	0.024
8	3.33	−2.35	30.14	34.23	64.37	11.0	0.004	0.023
9	2.42	1.54	34.03	35.14	69.16	1.45	0.017	0.014
10	3.52	−1.73	30.76	34.04	64.79	9.19	0.003	0.014

has only three conformations that contribute 98.9% of the electron transfer reactivity, and all have very similar conformations at the more crowded, smaller twist angle CNNC positions (shown at the bottom of the Newman projections down the NN bonds of Figure 2), while three orientations that are low enough in energy and have enough larger rate constants to contribute significantly to ET are calculated at the less crowded positions. The weighted effective barrier, $\lambda'_v(\text{eff}) = \sum_i f(i)\lambda'_v(i)$, is only 0.5 kcal/mol below that for the lowest-energy, largest contributor ($i = 1$). Figure 3 shows that the primary alkyl group substituted **Et$_2$N)$_2^{0/+}$** has many more conformations that contribute to λ'_v(eff), because multiple orientations at the more crowded as well as the less crowded alkyl group positions contribute. There is also a significantly larger spread in the resulting $\lambda'_v(i)$ values (Figure 1), which results in a 2.3 kcal/mol lower λ'_v(eff) than $\lambda'_v(1)$. We suggest that the result that the most stable conformations dominate ET reactions is common, and we have only used

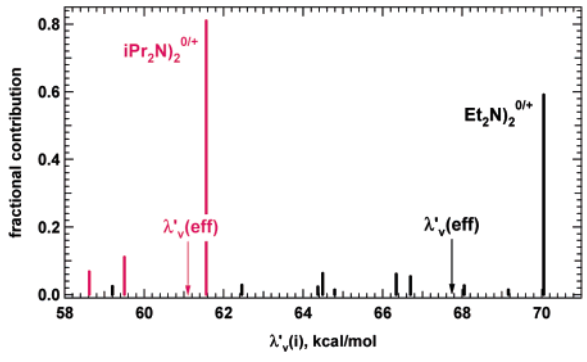

Figure 1. Plot of $f(i)$ versus $\lambda'_v(i)$ for **iPr$_2$N)$_2^{0/+}$** and **Et$_2$N)$_2^{0/+}$**.

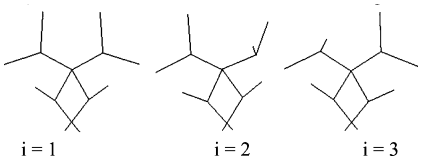

Figure 2. Newman projections down the NN bonds of the conformations of **iPr$_2$N)$_2^{0/+}$** that are calculated to contribute significantly to its ET reactions.

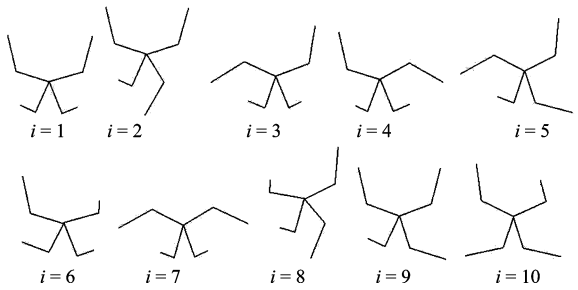

Figure 3. Newman projections down the NN bonds of the conformations of $\mathbf{Et_2N)_2}^{0/+}$ that are calculated to contribute significantly to its ET reactions.

the λ'_v value for the most stable neutral and radical cation conformations in calculating the λ'_v and H'_{ab} values of Table 2. This will be less true as conformational complexity increases, and we have not tried to obtain λ'_v values for a number of the compounds studied as a result. It will be noted that the entries in Table 3 differ slightly from the 6-31G* entries in Table 2 ($\lambda'_v(1)$ was obtained 0.34 kcal/mol higher for $\mathbf{iPr_2N)_2}^{0/+}$ and 0.12 kcal/mol lower for $\mathbf{Et_2N)_2}^{0/+}$ in Table 3 than in Table 2), presumably a result of using different programs and starting geometries.[14]

For the smaller couples in Table 2, the 6-31+G* basis set has been employed, but especially for larger low-barrier couples, we have used the considerably faster 6-31G* basis set that lacks diffuse functions. A larger λ'_v was calculated with the smaller 6-31G* basis set than with the 6-31+G* basis set for 19 of the 22 couples that were calculated both ways. The size of the difference depends on structure, with the largest differences for hydrazines being +3.07 kcal/mol for $\mathbf{[u6]Me_2}^{0/+}$ (45/2), +3.03 for $\mathbf{[6]Me_2}^{0/+}$ (44/2), and +2.43 for $\mathbf{Me_2N)_2}^{0/+}$ (18/3). Anomalously, the difference is −3.10 for $\mathbf{iPr_2N)_2}^{0/+}$ (1/2), leading to an unusually large difference in calculated $H'_{ab}(\Delta G^{\ddagger}_s) = 2.0$ between the two calculations of a factor of 2 see Table 2. The other 14 hydrazines calculated with both basis sets had a difference averaging 0.86 and a range of 1.79 to 0.17 kcal/mol. In contrast, the alkylated arylamines had differences of the opposite sign, −2.43 for $\mathbf{DMP}^{0/+}$ (27/3) and −0.42 for $\mathbf{TMPD}^{0/+}$ (10/3). The only compounds calculated using 6-31G* and 6-31+G* basis sets that have atoms with d electrons were $\mathbf{TTF}^{0/+}$ (18/2), difference of +1.46, and $\mathbf{TMTSF}^{0/+}$ (29/3), difference of 6.39 kcal/mol. The latter corresponds to a factor of 2.9 increase when diffuse functions are not included. $\mathbf{TMTSF}^{0/+}$ is obviously a very special case, both because of the presence of the much heavier selenium atoms and because an important qualitative difference in calculated geometry for the neutral form occurred. The huge change in calculated λ'_v occurs because the neutral oxidation level at 6-31G* optimizes as being significantly nonplanar, with a CSeCC angle of 17°, which is clearly not correct. The neutral form is calculated to be planar using the 6-31+G* basis set which includes diffuse functions.[15] λ'_v for $\mathbf{TMTSF}^{0/+}$ is clearly very small. Indeed, low-temperature superconductivity has been observed in several solid $(\mathbf{TMTSF}^{+})_2\mathbf{X}^{-}{}_2$ dimer radical cation salts.[16] It is not surprising that diffuse functions might be required to properly treat the heavy selenium atoms in **TMTSF**. An appropriate basis set for the ferrocene calculation (17/3) was chosen by our colleague, Clark Landis.

3. Modified Levich and Dogodnaze Equation. We consider here the analysis of the intrinsic rate constants k_{ii} obtained from our cross-reaction study. To interpret our data, we use simple modifications of the nonadiabatic rate equation of Levich and Dogodnaze.[17] The modifications that we introduced are as

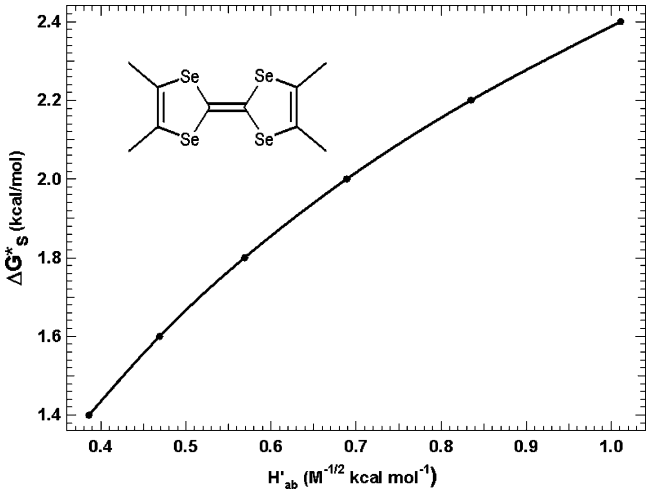

Figure 4. Plot of ΔG^{*}_s vs H'_{ab} for **TMTSF** from $k_{ii}(\text{fit}) = 1.57 \times 10^{11}$ M^{-1} s^{-1} ($\Delta G^{\ddagger}_{ii}(\text{fit}) = 2.18$ kcal/mol) and the calculated (UB3LYP/6-31+G*) λ'_v value of 3.40 kcal/mol.

follows: (a) the ΔG^* of classical Marcus−Hush two-state theory (eq 3) replaces $\lambda/4$ to allow consideration of

$$\Delta G^* = \lambda/4 - H_{ab} + (H_{ab})^2/\lambda \qquad (3)$$

reactions that do not have vanishingly small H_{ab} to be treated, and (b) the encounter complex formation constant, K_e, has been inserted so the equation can be used for intermolecular ET. This results in eq 4, which we will call the L&D equation. Like adiabatic Marcus theory

$$k_{L\&D}(25\ ^\circ\text{C}) = 1.52 \times 10^{14}\,(K_e H_{ab}{}^2/\lambda^{1/2}) \exp[-\Delta G^*/RT] \qquad (4)$$

eq 4 uses only λ and H_{ab} to predict the rate constant. Equation 4 retains the $H_{ab}{}^2$ dependence of the pre-exponential factor from nonadiabatic rate theory, because the pre-exponential factors clearly are not the same for all the compounds in the data set. It retains the activation barrier of classical theory and does not separate λ into high-frequency and low-frequency components. Although we are well aware that eq 4 is basically a graft of $H_{ab}{}^2$ dependence onto the pre-exponential factor of classical theory, all nonadiabatic theories that we have seen invoke $H_{ab}{}^2$ dependence of the pre-exponential factor. As will be developed below, use of eq 4 gives the result that intermolecular electron transfer reactions lie in the intermediate region between essentially adiabatic reactions (which may be achieved for intramolecular reactions through bridges with aromatic, C=C, and C≡C, or very few σ-bond bridges) and the essentially nonadiabatic reactions involved in photoelectron transfer, for which the Bixon−Jortner approach has been so successful.[2,3] As pointed out in the Introduction, our experimental data for intermolecular electron-transfer reactions cannot be rationalized using the Golden Rule approach, and eq 4 seems to us to be the smallest change from strictly classical theory that will rationalize the experimental data.

It is necessary to know both H_{ab} and K_e to extract ΔG^* (and hence λ) from intrinsic rate constants. There is, however, no good way of experimentally determining K_e values. Methods for calculating them that are suggested in the literature simply assume that for the encounter equilibrium ΔH° is zero,[1] which is unlikely to be true. Factors that raise H_{ab} appear likely to raise K_e as well. Interpretation of intermolecular reactions must include both factors, so we shall discuss $H'_{ab} = K_e{}^{1/2} H_{ab}$ (units,

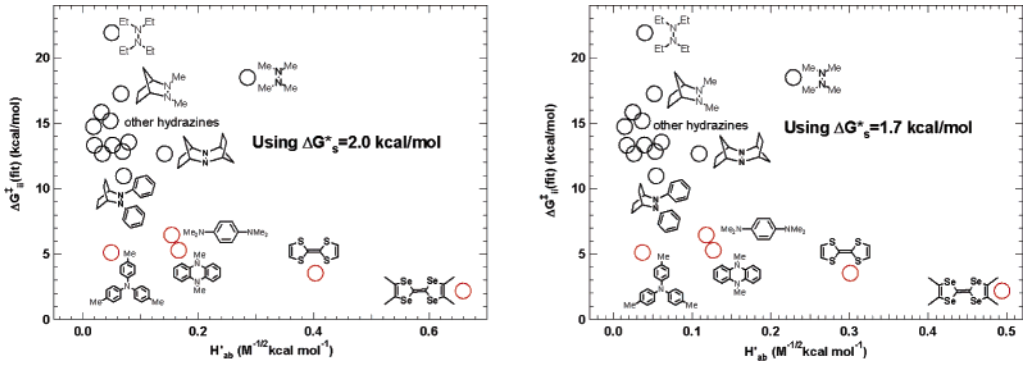

Figure 5. Plot of H'_{ab}values obtained from observed $\Delta G^{\ddagger}_{ii}$(fit) values assuming a constant ΔG^*_s of 2.0 kcal/mol (left panel) and of 1.7 (right panel).

$M^{-1/2}$ kcal mol^{-1}) and call them intrinsic electronic couplings, since they arise from intrinsic rate constants. If k_{ii}(fit) is substituted for $k_{L\&D}$(25 °C) in eq 3, the expression of eq 5 is obtained. We suggest that use of the L&D equation provides

$$\Delta G^* = 0.592\{32.655 - \ln[k_{ii}(\text{fit})] + \ln (H'_{ab})^2/\lambda^{1/2}\} \quad (5)$$

an internally consistent framework for interpretation of our data and allows partitioning of the observed reactivity into its ΔG^* and H'_{ab} components. Equations 3 and 5 contain two unknowns (λ and H'_{ab}), the experimentallly derived quantity, k_{ii}(fit), and the term ΔG^*, which can be estimated from a combination of DFT calculations and our estimates of ΔG^*_s as described below. Ideally, one would separate variables in the two equations and use the given k_{ii}(fit) value for a particular compound and its independently estimated ΔG^*, to calculate the related λ and H'_{ab} directly. However, it is not easy to separate the variables in the two equations, so instead this relationship along with an estimate of H'_{ab} is used to calculate λ. These values are then tried in eq 5, and H'_{ab} is iteratively varied until eq 5 is satisfied.

4. Estimation of ΔG^*_s. To extract H'_{ab} values from our data, we make the usual assumption that ΔG^* is the sum of solvent and internal vibrational terms and obtain the latter from the DFT calculations as $\Delta G^*_v = \lambda'_v/4$. Our best estimate of ΔG^*_s for these reactions is from the data for our lowest $\Delta G^{\ddagger}_{ii}$(fit) couple, **TMTSF**$^{0/+}$ (29/3). The 6-31+G* calculation gives a ΔG^*_v value of only 0.85 kcal/mol, so the Eyring barrier, $\Delta G^{\ddagger}_{ii}$(fit) = 2.2 kcal/mol, is dominated by ΔG^*_s, and ΔG^*_s is very unlikely to be more than about 2 kcal/mol.

By using eq 3 with eq 6, the k_{ii}(fit) ($\Delta G^{\ddagger}_{ii}$(fit)) for each couple for which λ'_v may be reliably calculated produces H'_{ab} values

$$\Delta G^* = [\lambda'_v(\text{DFT})/4] + \Delta G^*_s \quad (6)$$

that depend on ΔG^*_s. The observed k_{ii}(fit) value for **TMTSF** produces the ΔG^*_s versus H'_{ab} curve shown Figure 4. Obviously, changing the ΔG^*_s used changes the H'_{ab} value obtained. We compare plots for several couples using ΔG^*_s = 2.0 and 1.7 in Figure 5. Although there is not much correlation between $\Delta G^{\ddagger}_{ii}$(fit) and H'_{ab} except that the lowest barrier compounds have larger H'_{ab} values, these plots allow visual display of the data. Assuming constant ΔG^*_s values obviously makes the H'_{ab} values derived less accurate than if we could precisely evaluate ΔG^*_s. However, the fact that we observe no rate effects in our data that can be attributed to ΔG^*_s changes for different couples, even when significant changes are predicted using dielectric continuum theory, and the small value required for **TMTSF** suggest that a rather constant value near 2.0 kcal/mol is a reasonable estimate for these couples. As we have noted previously,[9] ΔG^*_s must be rather constant for tetra-*n*-alkylhydrazines with alkyl group length varying from two to six, so dielectric continuum theory, which predicts significant effects of molecular size, considerably overestimates these effects,[9] as has been concluded independently for very different reasons by Formosinho.[18] In the rest of this paper, we will discuss intrinsic electronic couplings obtained from k_{ii}(fit) and λ'_v values in terms of H'_{ab} (ΔG^*_s = 2.0) values for convenience. Although we do not know the best value to use and realize that decreasing ΔG^*_s would significantly contract the H'_{ab} range (see Figure 6), it would not change the order of intrinsic electronic couplings and hence would not change our conclusions.

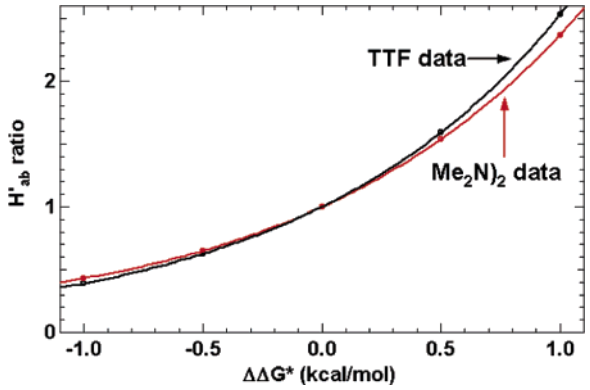

Figure 6. Effect of changing the ΔG^* estimate on the H'_{ab}obtained from an experimental $\Delta G^{\ddagger}_{ii}$(fit) value and λ_v(DFT) for **TTF** ($\Delta G^{\ddagger}_{ii}$(fit) = 3.5) and **Me$_2$N)$_2$** ($\Delta G^{\ddagger}_{ii}$(fit) = 18.5).

We next consider what sort of error in H'_{ab} will result from errors in calculated λ'_v, which affect the ΔG^* employed. A plot of the ratio of calculated H'_{ab} values as the ΔG^* estimate is changed is shown as Figure 6. Data are included representing a low-barrier couple, **TTF**$^{0/+}$ ($\Delta G^{\ddagger}_{ii}$(fit) = 3.5 kcal/mol) and a high-barrier one **Me$_2$N)$_2$**$^{0/+}$ ($\Delta G^{\ddagger}_{ii}$(fit) = 18.5 kcal/mol), to get an idea of the effect of barrier height on error. For both, we use the H'_{ab} calculated for ΔG^*_s = 2 kcal/mol with the λ'_v(DFT)/4 value as ΔG^*_v as $\Delta\Delta G^*$ = 0 and show how errors in computing ΔG_v(DFT), which appear as a change (Δ) in ΔG^*, affect the H'_{ab} obtained. It may be seen that there is only a slight increase in sensitivity as $\Delta G^{\ddagger}_{ii}$(fit) decreases and that the H'_{ab} estimate increases as the ΔG^* estimate increases. If ΔG^* is known to be ±1 kcal/mol (i.e., a 4 kcal/mol error in calculating λ'_v(DFT)), then H'_{ab} is established to within about a factor of 2.5(0.4) and at ±0.5 kcal/mol within a factor of 1.6-(0.6). We will just discuss the H'_{ab} (ΔG^*_s = 2.0) values here.

5. Hydrazine Couples. The principal factor affecting the electron-transfer barrier is obviously the reorganization energy of a couple, as demonstrated by the plot of $\Delta G^{\ddagger}_{ii}$(fit) versus

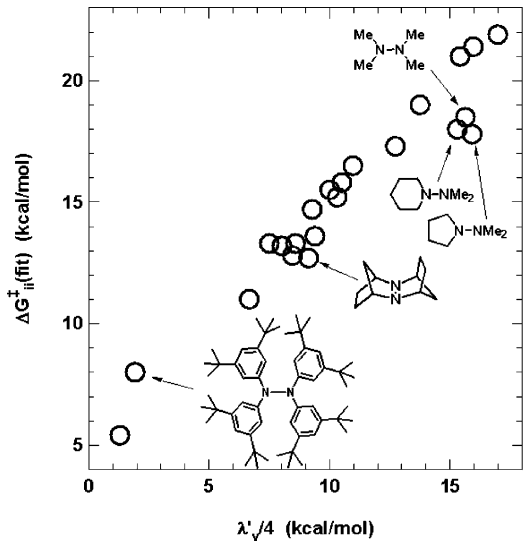

Figure 7. Plot of intrinsic electron-transfer barrier vs $\lambda'_v/4$ for 22 alkylated and arylated hydrazines.

$\lambda'_v/4$ shown in Figure 7, which includes the 22 hydrazine couples for which λ'_v values appear in Table 2. Their reactivity range is remarkable, a factor of 10^{12} in k_{ii}(fit), and as the plot shows, the great majority show an almost linear relationship. Nevertheless, there is definitely another factor because of the structure of the couples that lie furthest from the trend of the others. As discussed previously,[10,11] the three hydrazines that are clearly lower than the trend for the other compounds are those that are prevented from occupying the most stable conformation for *n*-alkylhydrazine radical cations, in which the alkyl groups block approach of a molecule to allow overlap with the two-atom NN π system, so that H'_{ab} is significantly larger than for compounds with ethyl or larger groups. The opposite deviation is shown by **b$_2$Ph$_2$N)$_2$** (33/2), for which approach to the aryl group π system is blocked by the eight *tert*-butyl groups, causing a significantly larger $\Delta G^{\ddagger}_{ii}$(fit) compared to its $\lambda'_v/4$ value than shown by the fastest hydrazine, **pTol$_2$N)$_2$** (32/2).

Figure 8 shows this effect visually, through plots of the ionization function projected onto the surface density function calculated using *Spartan '02* for four hydrazine radical cations that have increasing amounts of steric hindrance to approach the two-atom NN π system. The small methyl groups of **Me$_2$N)$_2$**$^+$ allow approach of another molecule to get significant overlap with the NN π system, but **Et$_2$N)$_2$**$^+$ does not, because it adopts the conformation indicated. It has the N−CH$_2$ bonds rotated to place two methyl groups that block approach to each face of the NN π system. The H'_{ab} ($\Delta G^* = 2$) values calculated correspond to a 34-fold drop in rate constant for ET. The value of 0.05 shown is that calculated for the minimum-energy 6-31+G* conformation, which may be somewhat too large.

Now that we have a better understanding of λ'_v through DFT calculations, it is clear that H'_{ab} is not as constant as we had previously suggested,[10,11] where we used H'_{ab} ($\Delta G^*_s = 2$) = 0.01 $M^{-1/2}$ kcal mol^{-1} for all hydrazines with all four alkyl groups larger than methyl, because we had no way of telling how H'_{ab} might change. Eleven of the tetraalkyl hydrazines that appear in Table 2 have H'_{ab} ($\Delta G^*_s = 2$) values in the range 0.02−0.08 $M^{-1/2}$ kcal mol^{-1}, all of which are substantially smaller than the values obtained for **Me$_2$N)$_2$**$^{0/+}$, **r6NNMe$_2$**$^{0/+}$, and **r5NNMe$_2$**$^{0/+}$; although the H'_{ab} ($\Delta G^*_s = 2$) value for the latter is about twice as large as we expected, and we doubt that we have found the proper conformations for minimizing λ'_v. The very easily deformed five-membered ring is a source of problems, because we lack a good way of generating conformations with the many energy minima that we suspect occur for it, and an intermediate value is found for **21/21**$^{0/+}$ (Figure 8). We have discussed conformations for **[6]Me$_2$**$^{0/+}$ and **[u6]Me$_2$**$^{0/+}$ previously,[11] as well as the difference between solution and gas-phase data.[19]

6. Tetrazene, Ferrocene, and Diamine Couples. The three 2-tetrazenes studied, **k33)$_2$N$_4$**$^{0/+}$ (55/1), **33)$_2$N$_4$**$^{0/+}$ (35/2), and **nPr$_4$N$_4$**$^{0/+}$, show faster electron transfer than any tetraalkyl, trialkylaryl, or dialkyldiaryl hydrazines studied, and the first two listed have λ'_v near 30 kcal/mol, slightly smaller than **22/tBuPh**$^{0/+}$ and larger than **22/Ph$_2$**$^{0/+}$, but substantially larger than **iPrPhN)$_2$**$^{0/+}$. These 2-tetrazenes share a four-atom π system that is smaller than that of most of the compounds studied except the hydrazines. Two of the three most deviant reactions in terms of k_{obsd}/k_{calcd} ratio involve 2-tetrazenes, and the single most deviant reaction is between **nPr$_4$N$_4$** and **33)$_2$N$_4$**$^+$ (ratio 5.6), making the rms deviations large for both of these couples. We have no particular explanation for this occurrence, and **k33)$_2$N$_4$**$^{0/+}$ has both a small rms deviation and the larger $\Delta G^{\ddagger}_{ii}$(fit) that is expected from the behavior of similar keto substitution on **33)$_2$PD**$^{0/+}$ and **33)$_2$N**$^{0/+}$. The dinitrogen "spacer" between the **k33N** groups apparently allows larger electronic interaction with approaching molecules than for branched hydrazines, from the H'_{ab} ($\Delta G^*_s = 2$) value of 0.20 $M^{-1/2}$ kcal mol^{-1} obtained for **k33)$_2$N$_4$** (Table 2).

Ferrocene (17/3) and dimethylferrocene (7/2) have similar $\Delta G^{\ddagger}_{ii}$(fit) values of 8.0 ± 0.3 kcal/mol. The range observed including the other two methylated ferrocenes studied previously[11] is smaller than that implied by reported self-exchange measurements, although we suggested from our measurements on pentamethylferrocene that the 10-fold larger rate constant reported for **FeCp*$_2$**$^{0/+}$ than **FeCp$_2$**$^{0/+}$ self-ET might be caused by a problem with the couple not being in the slow-exchange limit.[6] Weaver and co-workers assigned ferrocene and decamethylferrocene H_{ab} values of 0.1 and 0.2 kcal/mol, respectively, on the basis of solvent friction effects,[20] but they used a λ value for metallocene derivatives of 21.4 kcal/mol in acetonitrile and assumed that the λ_v value was in the range 2−4 kcal/mol for **FeCp$_2$**$^{0/+}$, so ΔG^*_s was assumed to be ≥4.3 kcal/mol, which is larger than is consistent with our data. As indicated in Table 2, if the B3LYP/LACV3P** level of theory λ'_v value of 4.5 kcal/mol is correct, an H'_{ab} ($\Delta G^*_s = 2$) value of 0.008 $M^{-1/2}$ kcal mol^{-1} is obtained. This value seems anomalously low, since it is about a factor of 5 lower than tetraalkylhydrazines with large enough substitutents to force ET to proceed through alkyl group interactions. However, as Weaver pointed out,[20] most of the hole in ferrocene is centered at the iron, which is sterically well protected from an approaching molecule.

We have only been able to study two amine couples because of lifetime problems for most amine radical cations. The two bicyclic diamines studied, **N[333]N** (28/3) and **N[222]N** (54/1), are calculated to have H'_{ab} ($\Delta G^*_s = 2$) values about an order of magnitude smaller than anything else studied. They are also rather different structurally, with the former having a 3e−σ $(NN)^+$ bond in its radical cation and the latter strong coupling of the nitrogen combination orbitals with the three CC bonds with which they are aligned. It appears as if these structural features substantially cut electronic interaction with the π-rich orbitals shared by the other systems, although only two cases of this sort have been studied.

7. Fastest Couples. Ten mono-triarylamine couples, generously supplied by H. B. Goodbrand,[21] are present in our data set. Although they are, as expected, at the upper end of the

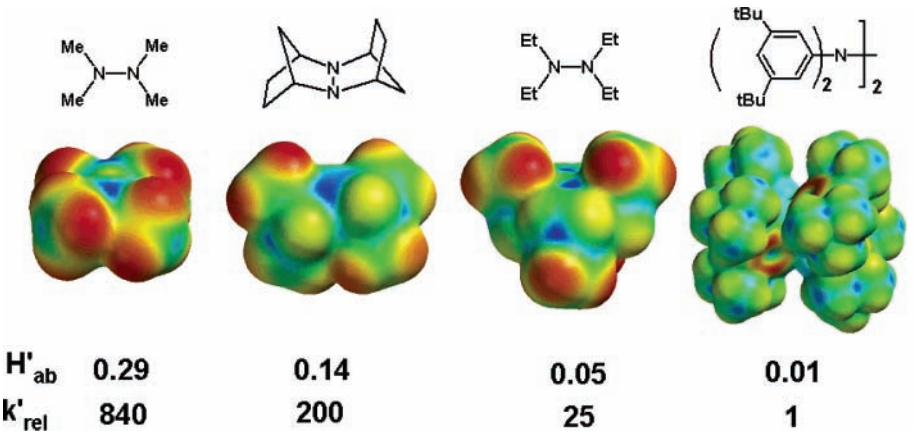

Figure 8. Ionization function mapped on the surface density function for UB3LYP/6-31G* calculations on (left to right) $\mathbf{Me_2N)_2}^+$ (18/3), $\mathbf{21/21}^+$ (6/3), $\mathbf{Et_2N)_2}^+$ (19/3), and $\mathbf{b_2Ph_2N)_2}^+$ (33/2), drawn at the same contour. The numbers labeled H'_{ab} are H'_{ab} ($\Delta G^* = 2$) ($M^{-1/2}$ kcal mol^{-1}) values, and those labeled k'_{rel} show how much a rate constant would change if the only effect were the change in H'_{ab}.

reactivity scale, they cover a $\Delta G^{\ddagger}_{ii}$(fit) range of over 3 kcal/mol, so they do vary in intrinsic reactivity. Triphenylamine has a 19-atom π system, which is hindered for approach near the nitrogen by the twisting of the aryl groups. $\mathbf{pTol_3N}^+$ (61/1) is the example with the best-established $\Delta G^{\ddagger}_{ii}$(fit) value, since it was studied for 6 reactions that agree well with each other. It has an H'_{ab} ($\Delta G^*_s = 2$) value of 0.06 $M^{1/2}$ kcal mol^{-1}, only 14% as large as that for $\mathbf{TMTSF}^{0/+}$(29/3) and within ± 0.03 $M^{-1/2}$ kcal mol^{-1} of the values obtained for hindered tetraalkylhydrazines. Eight other mono-triarylamines have $\Delta G^{\ddagger}_{ii}$(fit) values in the narrow range 5.20−5.00 kcal/mol, which are indistinguishable given the scatter in our data. $\mathbf{An_3N}$ (56/1) has an anomalously small $\Delta G^{\ddagger}_{ii}$(fit) value that is based on two reactions, those with $\mathbf{iPr_2N)_2}$ and $\mathbf{cHx_2N)_2}$, that give k_{calcd}/k_{obsd} values with $\Delta G^{\ddagger}$ differing by the anomalously large amount of 1.22 kcal/mol. If the slower rate constant was taken as the correct one (and they obviously both cannot be), it would make $\Delta G^{\ddagger}_{ii}$(fit) be 4.57 kcal/mol, and produce an H'_{ab} ($\Delta G^*_s = 2$) of 0.17 $M^{1/2}$ kcal mol^{-1}, which, although larger than any of the other triarylamines, seems more reasonable. Thus, even with the uncertainty in the $\mathbf{An_3N}$ data point, it seems hard to avoid the conclusion that electron-releasing substituents on the aromatic rings increase H'_{ab} (or that solvent effects change a lot and using $\Delta G^*_s = 2$ is insufficient for these larger molecules). There appears to be some evidence in these data that the electron-releasing *p*-methoxy substituent raises H'_{ab} (two of three largest H'_{ab} triarylamines in Table 2 are methoxylated) and the electron-withdrawing *p*-Br substitutent lowers it (the two lowest H'_{ab} triarylamines in Table 2 are brominated). This may be an echo of the clearer H'_{ab}-lowering effect of the electron-withdrawing 3-carbonyl groups on bicyclononyl-substituted systems. As suggested previously,[11] an electron-withdrawing group ought to make the electrophilic "hole" stay away from a region of the molecule, and since it is presumably the ability of electrons in the neutral component of the reaction to donate electrons to the hole in the cation that enhances H'_{ab}, the lack of hole character in the vicinity of electron-withdrawing groups might produce "dead spots" for ET approaches to such regions that effectively lower H'_{ab}. The effect may be principally at the para positions, because approach to the ortho positions is partially blocked by the adjacent rings. *p*-Phenyl and *p*-methoxy are calculated to raise the positive charge at the para position relative to that of tolyl rings (see Table 4).

An indication of the importance of steric lowering of H'_{ab} in triarylamines is given by comparing the value for the bis dianisylaminophenylene $\mathbf{An_4PD}^{0/+}$ (51/1) of 0.10 $M^{1/2}$ kcal mol^{-1} with that for its naphthalene analogue, $\mathbf{An_4ND}^{0/+}$ (60/1), 0.34 $M^{1/2}$ kcal mol^{-1}. The 1,4 substitution on a benzene ring for the former places the large $\mathbf{An_2N}$ substituents closer than the 2,6-naphthalene ring substitution for the latter, which apparently has the effect of blocking access to the aryl ring between the nitrogens. The compounds $\mathbf{Z_2An_2PD}^{0/+}$ (52/1) and $\mathbf{Z_4PD}^{0/+}$ (53/1) successively replace two and all four of the *p*-methyoxyphenyl substituents of $\mathbf{An_4PD}^{0/+}$ with the much bulkier *m*,*m*′-dianisylaminophenyl groups ("**Z**"). Although the barrier for $\mathbf{Z_2An_2PD}^{0/+}$ was indistinguishable from that of $\mathbf{An_4PD}^{0/+}$, the barrier for $\mathbf{Z_4PD}^{0/+}$ increases by about 1.4 kcal/mol, possibly reflecting the redox inversion between groups on the periphery and the interior suggested by the maker of these compounds, S. J. Blackstock.[22]

TABLE 4: Natural Population Analysis Charges for Ar_3N^+ Calculated Using UB3LYP/6-31G*

comp	para C_4	meta C_3 [a]	meta C_5
$\mathbf{(pAn)_3N}^+$	+0.37	−0.25	−0.30
$\mathbf{Xy_2PhN}^+$**:Ph ring**	+0.11	−0.20	−0.20
$\mathbf{Xy_2PhN}^+$**:Xy rings**	+0.03	−0.01	−0.21
$\mathbf{(pTol)_3N}^+$	+0.03	−0.21	−0.22
$\mathbf{(pBr)_3N}^+$	−0.10	−0.22	−0.22

[a] C_3 is syn to the methoxy methyl group and the methylated carbon for **Xy**.

TMTSF (29/3) has the smallest $\Delta G^{\ddagger}_{ii}$(fit) value and also the largest H'_{ab} ($\Delta G^*_s = 2.0$) of the compounds studied, 0.68 $M^{1/2}$ kcal mol^{-1}. The larger electronic couplings derived from our data are compared visually in Figure 9. We note that H'_{ab} consistently decreases as the overlap that a charge-bearing π system can achieve with an electron-transfer partner decreases. For the unhindered "aromatic compounds", we see a definite trend of Se > S > N for H'_{ab} as the row in the periodic table and hence radius of the charge-bearing heteroatoms is decreased. Changing the selenium atoms of **TMTSF** (29/3) to the sulfurs of **TTF** (18/2) without changing the π system size lowers H'_{ab} ($\Delta G^*_s = 2.0$) to 61% as large, and changing the heteroatoms to nitrogen in **DMP** (27/3) and **TMPD** (10/3) lowers it still further, to 23−26% that of **TMTSF**, despite the fact that the size of the π system is both larger (12 atoms for **DMP**) and smaller (8 atoms for **TMPD**) than the 10 atoms of **TMTSF**. The sulfur-containing $\mathbf{iPPT}^{0/+}$ (48/1) has H'_{ab} ($\Delta G^*_s = 2.0$) of 0.32 $M^{1/2}$ kcal mol^{-1}, distinctly larger than its dinitrogen analogue that has S replaced by NMe, $\mathbf{DMP}^{0/+}$, despite the fact that the former has a bulky *N*-isopropyl group.

Perhaps the most surprising aspect of our data set is the lack of a rate-slowing effect for replacing the methyls of $\mathbf{TMPD}^{0/+}$

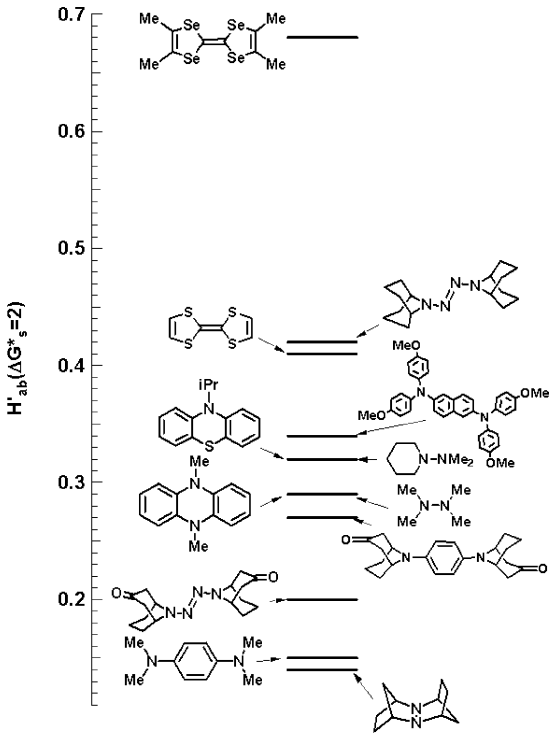

Figure 9. Comparison of the H'_{ab} ($\Delta G^*_s = 2.0$) values.

(10/3) by bicyclooctyl groups in going to **33)$_2$PD**$^{0/+}$ (15/3). The drop in $\Delta G^{\ddagger}_{ii}$(fit) that accompanies this structural change in hydrazines, **Me$_2$N)$_2$**$^{0/+}$ → **33N)$_2$**$^{0/+}$, is 4.9 kcal/mol, but this is principally caused by the change in NN rotation angle from nearly 90° to 180° as the bicycloalkyl groups are added. The increase in steric hindrance to the partner approach without changing NN bond twist angle for the change **Me$_2$N)$_2$**$^{0/+}$ → **Et$_2$N)$_2$**$^{0/+}$ raises $\Delta G^{\ddagger}_{ii}$(fit) by 3.4 kcal/mol. Although we expected a smaller increase for the **PD** derivatives because of their larger π systems and decreased steric hindrance in the middle of the molecule, with the *p*-phenylene "spacer", we did not anticipate the −0.2 kcal/mol $\Delta\Delta G^{\ddagger}_{ii}$(fit), which corresponds to equal ET reactivity within our experimental scatter for **TMPD**$^{0/+}$ and **33)$_2$PD**$^{0/+}$. The **33)$_2$PD**$^{0/+}$ intrinsic rate constant is based on only three reactions and might be considered suspect, but that for **k33)$_2$PD**$^{0/+}$ (16/2) is based on 21 reactions and is as well-established as any of our numbers. It corresponds to a $\Delta G^{\ddagger}_{ii}$(fit) value that is 0.7 kcal/mol higher than that for **TMPD**$^{0/+}$, while the H'_{ab} ($\Delta G^*_s = 2$) value is almost twice as large as that for **TMPD**$^{0/+}$, which we did not expect. We would have expected H'_{ab} ($\Delta G^*_s = 2$) to be significantly decreased upon increasing steric hindrance with the bicyclic alkyl groups, as it is for **Me$_2$N)$_2$**$^{0/+}$ (0.29 M$^{1/2}$kcal/mol) → **33)$_2$N**$^{0/+}$ (0.08 M$^{1/2}$kcal/mol), because significantly less contact with the π system appears likely for the bicycloalkylated **PD** derivative. Instead, the H'_{ab}($\Delta G^*_s = 2$) value obtained for **k33)$_2$PD**$^{0/+}$ increases to 0.37 M$^{1/2}$ kcal mol^{-1}. A rate-slowing "keto effect" like that observed for the hydrazines is apparently still present, with **k33)$_2$PD**$^{0/+}$ → **33)$_2$PD**$^{0/+}$ decreasing $\Delta G^{\ddagger}_{ii}$(fit) 0.8 kcal/mol and raising H'_{ab} ($\Delta G^*_s = 2$) to 0.37 M$^{1/2}$ kcal mol^{-1}.

Conclusions

Using cross-reaction rate constants and simple Marcus cross-rate theory works surprisingly well across a remarkably wide range of reactivities to extract useful estimates of self-exchange ET rate constants and their related activation energies. While we must conclude that our reactions are nonadiabatic and therefore that H_{ab} is an important factor in the observed reactivity, we remain puzzled that the Marcus cross-reaction relationship, eq 1, works so well. The electronic coupling H_{ab} is nearly impossible to access experimentally for intermolecular reactions because of the inseparability of λ_v, λ_s, and H_{ab} from rate constant measurements. Nonetheless, by using a combination of experiment, modern electron transfer theory, and structure−energy computations, it has been possible to separate these quantities and make estimates of H'_{ab} ($\Delta G^*_s = 2$) for a series of compounds with a very wide range of reactivity. While many of the H'_{ab} values obtained are not surprising—such as a relatively high H'_{ab} for compounds such as **TMTSF** or lower H'_{ab} for many tetraalkylhydrazines such as **Et$_2$N)$_2$**—there are others that appear to have truly counterintuitive values of H'_{ab}. For example, the relatively large H'_{ab} for **MeN$_2$)$_2$** compared to **Et$_2$N)$_2$** was unanticipated but can be understood in terms of differences in steric blocking by the alkyl groups.[11] It is clear that H'_{ab} increases down a family for a series of related compounds, Se > S > N, and while this trend may be intuitive, it has been possible to estimate the magnitude of this effect in a series of related compounds. It was somewhat surprising that the triarylamines and arylhydrazines, e.g., **22/tBuPh** and **22/Ph$_2$**, have H'_{ab} values nearly as low as those of unbranched tetraalkyl hydrazines, presumably as a result of their large π systems. It was also certainly not expected that **TMPD** would have a lower H'_{ab} than its significantly more sterically hindered **33)$_2$PD** and **k33)$_2$PD** analogues, and we see no explanation for this experimental result. We note that all the data that produce the H'_{ab} values quoted arise from cross-reactions and that the data for both very fast and very slow couples arise from reactions between the two types of compounds. Nevertheless, the majority of the H'_{ab} ($\Delta G^*_s = 2$) values reported make good sense; the interpretation given of this large set of data is quite internally consistent.

While it is inescapable that the primary factor governing intermolecular electron-transfer reactivity is the structural reorganization energy, λ_v, there are situations where H'_{ab} can have a significant impact, as for the increases in steric hindrance with little change in λ'_v, **Me$_2$N)$_2$**$^{0/+}$ → **Et$_2$N)$_2$**$^{0/+}$ (k_{ii}(fit) ratio 320) and **pTol$_2$N)$_2$**$^{0/+}$ → **b$_2$Ph$_2$N)$_2$**$^{0/+}$ (k_{ii}(fit) ratio 80, principally caused by H'_{ab} ($\Delta G^*_s = 2$) dropping from 0.06 to 0.01). Further, it is apparent from these results that λ_s is considerably lower than estimated by available theory and that there is a real need for improvement in computing this quantity. The failure of dielectric continuum theory to properly predict changes in λ_s has also been demonstrated by examining changes in intervalence transition energy (λ) for localized intervalence compounds,[23] so it occurs for both intramolecular photoelectron transfer and intermolecular thermal electron-transfer studied here. The inability to establish reliable estimates of λ_s is a fundamental limitation in the present interpretation, as it is for many condensed-phase dynamical studies.

Experimental Section

Data from the 65 new reactions in the data set are contained in Table 5 .

1. Computational Methodolgy. Nearly all radical ion geometries were optimized using standard gradient methods in *Spartan '02*[24] or the *Gaussian 98*[25] program suite. *Spartan '02* calculations were performed on a Dell Dimension 8250 2.53 GHz Pentium 4 computer with 1.00 GB RAM; *Gaussian 98* calculations were conducted on the Bohr cluster (dual, Intel Pentium III processors, 800 MHz, 256 KB cache) maintained by the chemistry departmental computing center at the Univer-

TABLE 5: The 65 New Reactions in the 206 Reaction Data Set, Observed (k_{ij}(obsd)) and Least Squares Calculated (k_{ij}(calcd)) Cross-Rate Constants, Their Ratio, and $\Delta\Delta G^{\ddagger}_{ij}$ Difference

entry	reductant	oxidant	k_{ij}(obsd) $M^{-1}\,s^{-1}$	k_{ij}(calcd) $M^{-1}\,s^{-1}$	ratio obsd/calcd	$\Delta\Delta G^{\ddagger}_{ij}$ kcal/mol
142	**[6]Me$_2$**(44)	**33)$_2$N$_4^+$**(35)	$1.4(1) \times 10^5$	1.1×10^5	1.27	−0.14
143	**21/Me$_2$**(46)	**22/Ph$_2^+$**(34)	$9.4(6) \times 10^4$	1.0×10^5	0.93	+0.05
144	**21/Me$_2$**(46)	**k33)$_2$PD$^+$**(16)	$1.5(1) \times 10^5$	1.0×10^5	1.47	−0.23
145	**21/Me$_2$**(46)	**33)$_2$N$_4^+$**(35)	$5.8(3) \times 10^4$	9.8×10^4	0.59	+0.31
146	**21/Me$_2$**(46)	**TTF$^+$**(18)	$6.5(6) \times 10^6$	3.9×10^6	1.67	−0.30
147	**Bz$_2$N)$_2$**(47)	**pTol$_2$N)$_2$**(32)	$2.3(3) \times 10^3$	3.9×10^3	0.59	+0.31
148	**Bz$_2$N)$_2$**(47)	**iPPT$^+$**(48)	$2.8(2) \times 10^4$	2.8×10^4	[1.0]	[0]
149	**Hy$_2$XY**(49)	**22/tBuPh$^+$**(23)	$1.8(2) \times 10^5$	1.6×10^5	1.14	−0.08
150	**Hy$_2$XY**(49)	**k33NN33$^+$**(13)	$3.2(2) \times 10^4$	3.7×10^4	0.88	+0.08
151	**BP$_2$6s**(50)	**k33)$_2$PD$^+$**(16)	$5.2(4) \times 10^6$	5.2×10^6	[1.0]	[0]
152	**An$_4$PD**(51)	**k33N)$_2^+$**(14)	$1.19(2) \times 10^6$	1.2×10^6	1.03	−0.02
153	**iPr$_2$N)$_2$**(1)	**An$_4$PD$^+$**(51)	$8.1(3) \times 10^3$	1.0×10^4	0.80	+0.13
154	**cHx$_2$N)$_2$**(11)	**An$_4$PD$^+$**(51)	$4.7(4) \times 10^4$	3.1×10^4	1.52	−0.25
155	**k33N)$_2$**(14)	**PAP)$_2$PD$^+$**(52)	$3.1(2) \times 10^5$	3.9×10^5	0.79	+0.14
156	**cHx$_2$N)$_2$**(11)	**PAP)$_2$PD$^+$**(52)	$7.5(6) \times 10^5$	3.8×10^5	1.99	−0.41
157	**cHx$_2$N)$_2$**(11)	**MAP)$_2^+$**(53)	$1.86(5) \times 10^5$	1.6×10^5	1.13	−0.07
158	**N[222]N**(54)	**b$_2$Ph$_2$N)$_2^+$**(33)	$4.3(5) \times 10^5$	4.3×10^5	[1.0]	[0]
159	**cHx$_2$N)$_2$**(11)	**An$_3$N$^+$**(56)	$1.3(1) \times 10^7$	4.7×10^6	2.77	0.60
160	**iPr$_2$N)$_2$**(1)	**An$_3$N$^+$**(56)	$5.7(2) \times 10^5$	1.6×10^6	0.36	0.61
161	**21/Me$_2$**(46)	**FeCp′$_2^+$**(7)	$2.3(1) \times 10^4$	3.1×10^4	0.75	0.17
162	**iPr$_2$N)$_2$**(1)	**k33)$_2$N$_4^+$**(55)	$8.8(6) \times 10^4$	7.1×10^4	1.24	−0.13
163	**cHx$_2$N)$_2$**(11)	**k33)$_2$N$_4^+$**(55)	$1.5(2) \times 10^5$	2.1×10^5	0.73	+0.19
164	**Bz$_2$N)$_2$**(47)	**k33)$_2$N$_4^+$**(55)	$3.0(2) \times 10^2$	2.7×10^2	1.13	−0.07
165	**[u6]Me$_2$**(45)	**An$_4$PD$^+$**(51)	$3.2(1) \times 10^4$	3.8×10^4	0.85	+0.09
166	**[6]Me$_2$**(44)	**An$_4$PD$^+$**(51)	$8.8(2) \times 10^5$	1.7×10^6	0.50	+0.41
167	**An$_4$PD**(51)	**k33N)$_2^+$**(14)	$4.4(3) \times 10^4$	2.4×10^4	1.86	−0.37
168	**r6NNr5**(57)	**k33N)$_2^+$**(14)	$6.7(3) \times 10^2$	1.2×10^3	0.57	+0.33
169	**r6NNr5**(57)	**k33)$_2$PD $^+$**(16)	$1.47(4) \times 10^5$	8.4×10^4	1.75	−0.33
170	**nPr$_4$N$_4$**(58)	**k33N)$_2^+$**(14)	$2.0(1) \times 10^4$	4.6×10^4	0.43	+0.50
171	**nPr$_4$N$_4$**(58)	**22/Ph$_2^+$**(34)	$1.5(1) \times 10^6$	3.6×10^6	0.41	+0.52
172	**nPr$_4$N$_4$**(58)	**33)$_2$N$_4^+$**(35)	$1.8(3) \times 10^7$	3.2×10^6	5.62	−1.02
173	**Bz$_2$N)$_2$**(47)	**pBr)$_3$N$^+$**(59)	$4.6(6) \times 10^7$	4.6×10^7	[1.0]	[0]
174	**iPr$_2$N)$_2$**(1)	**MAP$_2$PD$^+$**(53)	$4.5(2) \times 10^4$	5.5×10^4	0.82	+0.12
175	**u6Me$_2$**(45)	**PAP$_2$PD$^+$**(52)	$3.4(2) \times 10^5$	4.7×10^5	0.72	0.19
176	**iPr$_2$N)$_2$**(1)	**PAP$_2$PD$^+$**(52)	$1.1(1) \times 10^5$	1.3×10^5	0.88	+0.08
177	**u6Me$_2$**(45)	**MAP$_2$PD$^+$**(53)	$2.2(1) \times 10^5$	2.0×10^5	1.07	−0.04
178	**iPr$_2$N)$_2$**(1)	**An$_4$ND$^+$**(60)	$2.3(2) \times 10^5$	2.4×10^5	0.96	+0.03
179	**u6Me$_2$**(45)	**An$_4$ND$^+$**(60)	$5.7(3) \times 10^5$	9.0×10^5	0.63	+0.27
180	**cHx$_2$N)$_2$**(11)	**An$_4$ND$^+$**(60)	$8.3(5) \times 10^5$	7.2×10^5	1.15	−0.08
181	**(k33N)$_2$**(14)	**An$_4$ND$^+$**(60)	$1.03(6) \times 10^6$	7.2×10^5	1.43	−0.21
182	**iPr$_2$N)$_2^0$**(1)	**pTol$_3$N$^+$**(61)	$1.4(3) \times 10^7$	9.5×10^6	1.47	−0.23
183	**iPrPhN)$_2$**(62)	**pTol$_3$N$^+$**(61)	$2.8(5) \times 10^7$	2.8×10^7	[1.0]	[0]
184	**k33)$_2$N$_4^+$**(55)	**pTol$_3$N$^+$**(61)	1.41×10^7	1.4×10^7	0.99	+0.01
185	**Bz$_2$N)$_2$**(47)	**pTol$_3$N$^+$**(61)	4.4×10^4	5.0×10^4	0.89	+0.07
186	**nHx$_2$N)$_2^{0/+}$**(21)	**pTol$_3$N$^+$**(61)	4.20×10^6	4.4×10^6	0.96	+0.02
187	**nPr$_2$N)$_2^0$**(20)	**pTol$_3$N$^+$**(61)	2.14×10^6	2.7×10^6	0.80	+0.14
188	**Bz$_2$N)$_2$**(47)	**Xy$_2$pBrN^0**(63)	1.15×10^5	5.7×10^4	2.03	-0.42
189	**cHx$_2$N)$_2$**(11)	**Xy$_2$pBrN^0**(63)	8.10×10^6	2.5×10^7	0.32	+0.67
190	**nPr$_2$N)$_2^0$**(20)	**Xy$_2$pBrN^0**(63)	4.30×10^6	2.6×10^6	1.63	−0.29
191	**Bz$_2$N)$_2$**(47)	**Xy$_2$pTolN^0**(64)	2.6×10^4	2.6×10^4	[1.0]	[0]
192	**Bz$_2$N)$_2$**(47)	**Xy$_2$pBiN^0**(65)	6.9×10^4	8.0×10^4	0.86	+0.09
193	**nPr$_2$N)$_2^0$**(20)	**Xy$_2$pBiN^0**(65)	3.7×10^6	4.3×10^6	0.87	+0.09
194	**nHx$_2$N)$_2^{0/+}$**(21)	**Xy$_2$pBiN^0**(65)	9.2×10^6	6.9×10^6	1.33	−0.17
195	**Bz$_2$N)$_2$**(47)	**XypBi$_2$N^0**(66)	2.2×10^5	2.2×10^6	[1.0]	[0]
196	**Bz$_2$N)$_2$**(47)	**XyptBu$_2$N^0**(67)	4.6×10^4	4.7×10^4	0.99	+0.01
197	**nPr$_2$N)$_2^0$**(20)	**XyptB$_2$N^0**(67)	2.6×10^6	2.6×10^6	1.01	−0.01
198	**Bz$_2$N)$_2$**(47)	**PhpTol$_2$N^0**(68)	3.0×10^4	3.0×10^4	[1.0]	[0]
199	**nPr$_2$N)$_2^0$**(20)	**Xy$_2$ptBuN^0**(69)	1.5×10^6	1.7×10^6	0.90	0.06
200	**Bz$_2$N)$_2$**(47)	**Xy$_2$ptBuN^0**(69)	3.1×10^4	2.8×10^4	1.12	−0.07
201	**nPr$_2$N)$_2^0$**(20)	**Xy$_2$AnN^0**(70)	5.2×10^5	5.3×10^5	0.98	0.01
202	**iPr$_2$N)$_2^0$**(1)	**Xy$_2$AnN^0**(70)	2.3×10^6	2.0×10^6	1.16	−0.09
203	**Bz$_2$N)$_2$**(47)	**Xy$_2$AnN^0**(70)	5.9×10^3	6.8×10^3	0.87	0.08
204	**nPr$_2$N)$_2^0$**(20)	**Xy$_2$pOPh^0**(71)	1.1×10^6	1.1×10^6	1.01	−0.004
205	**Bz$_2$N)$_2$**(47)	**Xy$_2$pOPh^0**(71)	1.7×10^4	1.7×10^4	0.99	−0.004
206	**Bz$_2$N)$_2$**(47)	**XyAn$_2$N^0**(72)	2.1×10^3	2.1×10^3	[1.0]	[0]

sity of Wisconsin. In the case of hydrazines containing multiple phenyl groups, the SCF=QC algorithm was required to aid convergence. Exceptions to this were ferrocene calculations, which used *Jaguar*,[26] and cc-pVDZ[27] basis set calculations, which used the *Gaussian 03*[28] program suite. Frequency analyses were carried out using *Gaussian 98* to ensure that the structures lay on a minimum on the potential energy surface. The SCF=TIGHT keyword was added to all single-point calculations in order to maintain consistency, as this is recommended for any single point using the 6-31+G* basis set. All calculations

employed the standard Pople-style 6-31G* or 6-31+G* basis sets as implemented in Spartan and Gaussian, and the B3LYP[29] density functional was applied in each case unless otherwise mentioned.

Acknowledgment. We thank the National Science Foundation for financial support of this work under grant CHE-0240197 (to S.F.N.) and CHE-0072928 (to J.R.P.). We thank H. Bruce Goodbrand (Xerox Research Centre of Canada) and Silas J. Blackstock (University of Alabama) for generously supplying many of the triarylamine derivatives used in this work. We thank Kathleen Fitzpatrick for Spartan calculations of many rotational isomers of $\mathbf{Et_2N)_2}^{0/+}$ that were helpful in locating the ones used here to calculate λ'_v. We thank Prof. Clark Landis (University of Wisconsin) for the ferrocene calculations, which used the program *Jaguar* on his cluster. M.N.W. wishes to thank Dr. Peter A. Petillo for useful discussions.

Note Added after Print Publication. Author Yun Luo was not included in the version of this Article published on Articles ASAP on September 26, 2006, and printed in the October 19, 2006, issue (Vol. 110, No. 41, pp 11655−11676). The corrected electronic version was posted on December 6, 2006, and an Addition and Correction appears in the December 28, 2006, issue (Vol. 110, No. 51).

Supporting Information Available: Additional experimental data and DFT calculations. This material is available free of charge via the Internet at http://pubs.acs.org.

References and Notes

(1) Marcus, R. A.; Sutin, N. *Biochim. Biophys. Acta* **1985**, *811*, 265. (b) Sutin, N. *Prog. Inorg. Chem.* **1983**, *30*, 441.

(2) Bixon, M.; Jortner, J. *Adv. Chem. Phys.* **1999**, *106*, 35−202 (see p 52).

(3) Closs, G. L.; Calcaterra, L. T.; Green, N. J.; Penfield, K. W.; Miller, J. R. *J. Phys. Chem.* **1986**, *90*, 3673−3683.

(4) Closs, G. L.; Miller, J. R. *Science* **1988**, *240*, 440−448.

(5) Nelsen, S. F.; Wang, Y.; Ramm, M. T.; Accola, M. A.; Pladziewicz, J. R. *J. Phys. Chem.* **1992**, *96*, 10654−10658.

(6) Nelsen, S. F.; Chen, L.-J.; Ramm, M. T.; Voy, G. T.; Powell, D. R.; Accola, M. A.; Seehafer, T.; Sabelko, J.; Pladziewicz, J. R. *J. Org. Chem.* **1996**, *61*, 1405−1412.

(7) Nelsen, S. F.; Ismagilov, R. F.; Chen, L.-J.; Brandt, J. L.; Chen, X.; Pladziewicz, J. R. *J. Am. Chem. Soc.* **1996**, *118*, 1555−1556.

(8) Nelsen, S. F.; Ramm, M. T.; Ismagilov, R. F.; Nagy, M. A.; Trieber, D. A., II; Powell, D. R.; Chen, X.; Gengler, J. J.; Qu, Q.; Brandt, J. L.; Pladziewicz, J. R. *J. Am. Chem. Soc.* **1997**, *119*, 5900−5907.

(9) Nelsen, S. F.; Ismagilov, R. F.; Gentile, K. E.; Nagy, M. A.; Tran, H. Q.; Qu, Q.; Halfen, D. T.; Oldegard, A. L.; Pladziewicz, J. R. *J. Am. Chem. Soc.* **1998**, *120*, 8230−8240.

(10) Nelsen, S. F.; Trieber, D. A., II; Nagy, M. A.; Konradsson, A.; Halfen, D. T.; Splan, K. A.; Pladziewicz, J. R. *J. Am. Chem. Soc.* **2000**, *122*, 5940−5946.

(11) Nelsen, S. F.; Pladziewicz, J. R. *Acct. Chem. Res.* **2002**, *35*, 247−254.

(12) Nelsen, S. F.; Blackstock, S. C.; Kim, Y. *J. Am. Chem. Soc.* **1987**, *109*, 677−682.

(13) Values used were $\mathbf{iPr_2N)_2}^{0/+}$: $\mathbf{c}^+$, −583.3752050 au; $\mathbf{c}^0$, −583.5367185. $\mathbf{Et_2N)_2}^{0/+}$: $\mathbf{c}^+$, −426.130622; $\mathbf{c}^0$, −426.2997692.

(14) It appears that only energy-minimum conformations should be Boltzmann-averaged. When we stepped the smaller CNNC angle of $\mathbf{Me_2N)_2}$ in 5° increments to generate a series of increasingly less stable nonminimum neutral structures and weighted their contributions in a manner similar to that used for the energy-minimum conformations of the compounds discussed above, the decrease in λ'_v outweighed the effect of the increase in enthalpy and caused most of the calculated reactivity to occur from significantly lower λ'_v structures that caused a large lowering of the averaged λ'_v. This effect was large enough that the H'_{ab} lowering effect of ethyl substitution largely disappeared, along with the rationalization of why $\mathbf{Me_2N)_2}$ is significantly more reactive than $\mathbf{Et_2N)_2}$ in ET reactions. Thus, although we are not very sure why, it seems clear that only minimum-energy conformations ought to be considered as contributing significantly to the rate constant in this sort of treatment.

(15) See the Supporting Information for further discussion of the basis set effect on this system.

(16) Williams, J. M.; Beno, M. A.; Wang, H. H.; Leung, P. C. W.; Emge, T. J.; Geiser, U.; Carlson, K. D. *Acc. Chem. Res.* **1985**, *18*, 261−267.

(17) Modified from eq 3(6) of ref 2.

(18) Formosinho, J. J.; Arnault, L. G.; Fausto, R. *Prog. React. Kinet.* **1998**, *23*, 1−90.

(19) Nelsen, S. F.; Konradsson, A.; Jentzsch, T. L.; O'Konek, J. J.; Pladziewicz, J. R. *J. Chem. Soc., Perkin Trans. 2* **2001**, 1552−1556.

(20) McMannis, G. E.; Nielson, R. M.; Gochev, A.; Weaver, M. J. *J. Am. Chem. Soc.* **1989**, *111*, 5533−5541.

(21) Goodbrand, H. B.; Hu, N.-X. *J. Org. Chem.* **1999**, *64*, 670−674.

(22) Selby, T. D.; Blackstock, S. C. *J. Am. Chem. Soc.* **1998**, *120*, 12155−12157.

(23) Nelsen, S. F.; Trieber, D. A., II; Ismagilov, R. F.; Teki, Y. *J. Am. Chem. Soc.* **2001**, *123*, 5684−5694.

(24) *Spartan '02*; Wavefunction, Inc., Irvine, CA.

(25) Frisch, M. J.; Trucks, G. W.; Schlegel, H. B.; Scuseria, G. E.; Robb, M. A.; Cheeseman, J. R.; Zakrzewski, V. G.; Montgomery, J. A., Jr.; Stratmann, R. E.; Burant, J. C.; Dapprich, S.; Millam, J. M.; Daniels, A. D.; Kudin, K. N.; Strain, M. C.; Farkas, O.; Tomasi, J.; Barone, V.; Cossi, M.; Cammi, R.; Mennucci, B.; Pomelli, C.; Adamo, C.; Clifford, S.; Ochterski, J.; Petersson, G. A.; Ayala, P. Y.; Cui, Q.; Morokuma, K.; Malick, D. K.; Rabuck, A. D.; Raghavachari, K.; Foresman, J. B.; Cioslowski, J.; Ortiz, J. V.; Stefanov, B. B.; Liu, G.; Liashenko, A.; Piskorz, P.; Komaromi, I.; Gomperts, R.; Martin, R. L.; Fox, D. J.; Keith, T.; Al-Laham, M. A.; Peng, C. Y.; Nanayakkara, A.; Gonzalez, C.; Challacombe, M.; Gill, P. M. W.; Johnson, B. G.; Chen, W.; Wong, M. W.; Andres, J. L.; Head-Gordon, M.; Replogle, E. S.; Pople, J. A. *Gaussian 98*, revision A.9; Gaussian, Inc.: Pittsburgh, PA, 1998.

(26) *Jaguar*, version 4.2; release 73.

(27) Wilson, A. K.; Woon, D. E.; Peterson, K. A.; Dunning, T. H., Jr. *J. Chem. Phys.* **1999**, *110*, 7667−7676.

(28) Frisch, M. J.; Trucks, G. W.; Schlegel, H. B.; Scuseria, G. E.; Robb, M. A.; Cheeseman, J. R.; Montgomery, J. A., Jr.; Vreven, T.; Kudin, K. N.; Burant, J. C.; Millam, J. M.; Iyengar, S. S.; Tomasi, J.; Barone, V.; Mennucci, B.; Cossi, M.; Scalmani, G.; Rega, N.; Petersson, G. A.; Nakatsuji, H.; Hada, M.; Ehara, M.; Toyota, K.; Fukuda, R.; Hasegawa, J.; Ishida, M.; Nakajima, T.; Honda, Y.; Kitao, O.; Nakai, H.; Klene, M.; Li, X.; Knox, J. E.; Hratchian, H. P.; Cross, J. B.; Bakken, V.; Adamo, C.; Jaramillo, J.; Gomperts, R.; Stratmann, R. E.; Yazyev, O.; Austin, A. J.; Cammi, R.; Pomelli, C.; Ochterski, J. W.; Ayala, P. Y.; Morokuma, K.; Voth, G. A.; Salvador, P.; Dannenberg, J. J.; Zakrzewski, V. G.; Dapprich, S.; Daniels, A. D.; Strain, M. C.; Farkas, O.; Malick, D. K.; Rabuck, A. D.; Raghavachari, K.; Foresman, J. B.; Ortiz, J. V.; Cui, Q.; Baboul, A. G.; Clifford, S.; Cioslowski, J.; Stefanov, B. B.; Liu, G.; Liashenko, A.; Piskorz, P.; Komaromi, I.; Martin, R. L.; Fox, D. J.; Keith, T.; Al-Laham, M. A.; Peng, C. Y.; Nanayakkara, A.; Challacombe, M.; Gill, P. M. W.; Johnson, B.; Chen, W.; Wong, M. W.; Gonzalez, C.; Pople, J. A. *Gaussian 03*, revision B.05; Gaussian, Inc.: Pittsburgh, PA, 2003.

(29) Becke, A. D. *J. Chem. Phys.* **1993**, *98*, 5648. (b) Becke, A. D. *Phys. Rev. A* **1988**, *38*, 3098. (c) Lee, C.; Yang, W.; Parr, R. G. *Phys. Rev. B* **1988**, *37*, 785. (d) Vosko, S. H.; Wilk, S. H.; Nusair, M. *Can. J. Phys.* **1980**, *58*, 1200.